Ligand-free Nickel-catalyzed carboxylate *O*-arylation: Mechanistic insight into Ni^{I}/Ni^{III} cycles

Lukas A. Wolzak,[1] Felix J. de Zwart,[1] Jean-Pierre H. Oudsen,[1] Stuart A. Bartlett,[2] Bas de Bruin,[1] Joost N.H. Reek,[1,*] Moniek Tromp,[3,*] and Ties J. Korstanje[1,*]

1) Homogeneous, Supramolecular and Bio-Inspired Catalysis Group, van 't Hoff Institute for Molecular Sciences (HIMS), University of Amsterdam, Science Park 904, 1098XH Amsterdam, The Netherlands. 2) Diamond Light Source, Harwell Science and Innovation Campus, Didcot, Oxfordshire, OX11 0DE, UK. 3) Materials Chemistry, Zernike Institute for Advance Materials, University of Groningen, Nijenborgh 4, 9747AG Groningen, The Netherlands.

Corresponding authors: t.j.korstanje@uva.nl; Moniek.tromp@rug.nl; j.n.h.reek@uva.nl

KEYWORDS: Nickel catalysis, C-heteroatom bond formations, carboxylate O-arylation.

Abstract: Nickel-catalyzed cross-coupling reactions have become a powerful methodology to construct C–heteroatom bonds. However, many protocols suffer from competitive off-cycle reaction pathways and require non-equimolar amounts of coupling partners to suppress them. Here, we report on mechanistic examination of carboxylate *O*-arylation under thermal conditions, in both the presence and absence of an exogeneous bipyridine-ligand. Furthermore, spectroscopic studies of the novel ligand-free carboxylate *O*-arylation reaction unveiled the resting state of the nickel catalyst, the crucial role of the alkylamine base and the formation of a catalytically relevant Ni^{I}–Ni^{II} dimer upon reduction. This study provides insights into the competition between productive catalysis and deleterious pathways (comproportionation and protodehalogenation) that exist for all elementary steps in the commonly proposed self-sustained Ni^{I}/Ni^{III} catalytic cycle. Thereby we show that for productive nickel-catalyzed carboxylate *O*-arylation a choice must be made between either mild conditions or equimolar ratios of substrates.

Introduction

In recent years, nickel catalysis has enabled the formation of challenging C–heteroatom bonds, resulting in previously elusive cross-coupling reactions that can now be performed under mild conditions.[1–3] An example hereof is the coupling of carboxylic acids and aryl halides to form *O*-aryl esters enabled by (dtbbpy)NiX_2 under photochemical[4–8], electrochemical[9] or thermal reaction conditions[10] (Figure 1A). This cross-coupling reaction is notably demanding due to the low nucleophilicity of the carboxylate group. Although analogous *O*-aryl ester bond formation reactions catalyzed by palladium have been reported, these protocols are far from mild and efficient, and are relying on stoichiometric amounts of silver salts.[11,12] Mechanistically, nickel-catalyzed C–heteroatom bond formations under thermal conditions were proposed to proceed via a self-sustained Ni^{I}/Ni^{III} catalytic cycle.[10] In addition, the relevance of this catalytic mechanism was also demonstrated under photochemical[13–17] and electrochemical[14] reaction conditions. From these catalytic studies it became apparent that in order to successfully engage a self-sustained Ni^{I}/Ni^{III} catalytic cycle the continuous reduction of Ni^{II} to Ni^{I} is required, as Ni^{I} is prone to deactivation via an exergonic comproportionation reaction with Ni^{III} forming inactive Ni^{II}. Besides catalytic studies, another important approach to elucidate catalytic pathways has been provided by the synthesis, characterization and *in situ* generation of Ni^{I} complexes and the study of their reactivity. Investigations have unveiled that specific Ni^{I} complexes

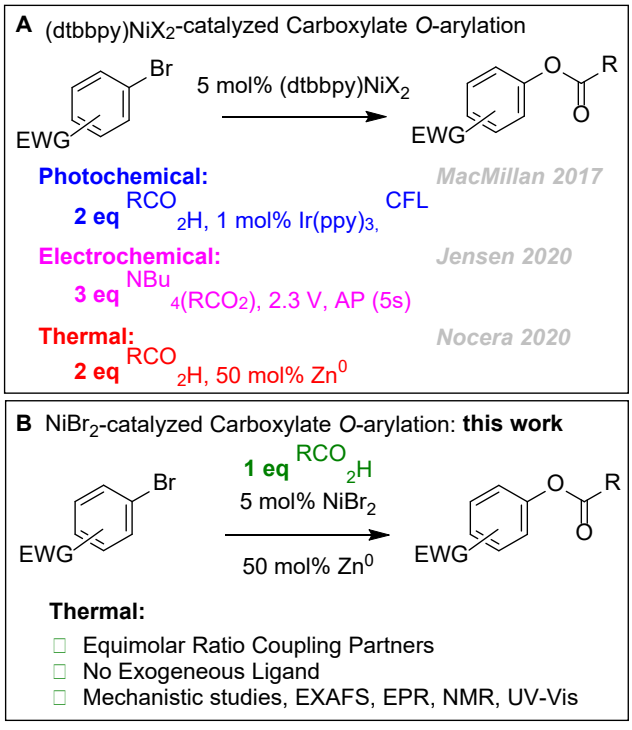

Figure 1. Nickel Catalyzed Cross-Coupling between aryl halides and carboxylic acids using A) (dtbbpy)NiX_2 system or B) Ligand-Free system. (dtbbpy = 4,4'-di-tert-butyl-2,2'-bipyridine, AP = alternating polarity).

bearing a bipyridine (bpy) based ligand[14,18–20] are indeed able to activate aryl halides[14,19] and that the required Ni^{III} state can be accessed via oxidative addition of a Ni^{I} complex.[21,22] So far mechanistic insights through catalytic studies and stoichiometric reactions have demonstrated the validity of the elementary steps proposed in the self-sustained Ni^{I}/Ni^{III} catalytic cycle. However, they do not account for the non-equimolar ratios of substrates often required for productive C–heteroatom bond formations. Therefore, to further develop the field of nickel cross-coupling and enable more efficient reactions, a better understanding of the competition between productive fundamental elementary steps and off-cycle reaction pathways is required.

Here, we report on a detailed mechanistic study, where carboxylate *O*-arylation is performed under thermal and photocatalytic conditions in both the presence and absence of a dtbbpy-ligand and show ligand-free conditions (i.e. no exogeneous dtbbpy-ligand) enable an equimolar ratio of coupling partners (Figure 1B). In addition, the nickel complexes prior and after reduction have been studied with a variety of spectroscopic techniques, which show the first observation of a Ni^{I}–Ni^{II} dimer after reduction under ligand-free conditions. Moreover, a scope of coupling of carboxylic acids with aryl bromides is displayed using substoichiometric amounts of earth-abundant zinc as reductant and nickel(II) bromide as catalyst. Overall, we provide insight into self-sustained Ni^{I}/Ni^{III} catalytic cycles including deleterious off-cycle reaction pathways and show that for nickel-catalyzed carboxylate *O*-arylation a choice must be made between either mild conditions or equimolar ratios of substrates.

Results and discussion

Approach. Ligand-free protocols have been reported for nickel-catalyzed C–N cross-coupling reactions,[23,24] and therefore a similar approach to carboxylate *O*-arylation could be feasible. After initial optimization (Table S1–S4) we arrived at optimal reaction conditions furnishing *O*-aryl ester, 4'-benzoyloxyacetophenone (**2**) in 81% yield without use of an exogeneous ligand (Table 1, entry 1). First, a hypothesis (Figure 2) on the mechanism of this reaction and the structure of nickel complexes relevant to it was developed through catalytic studies as described in the following section, after which the proposed mechanism was corroborated through spectroscopic studies (Figure 3) in the last section.

Catalytic studies. To establish that ligand-free carboxylate *O*-arylation indeed operates via a self-sustained Ni^{I}/Ni^{III} catalytic cycle, dependency on photons was excluded (Table 1, entry 2). Furthermore, the bulk of nickel is proposed to remain in a dormant Ni^{II} oxidation state (precatalyst, Figure 2) which was supported experimentally by a dependency of the rate of product formation on the reduction by zinc (Figure S2). To indicate oxidative addition as an elementary step in the mechanism a strong rate dependency on the electronic parameter of the aryl bromides (Hammett Plot, Figure S3) was found, similar to (dtbbpy)$NiBr_2$-catalyzed reactions.

Table 1. Nickel-catalyzed carboxylate *O*-arylation

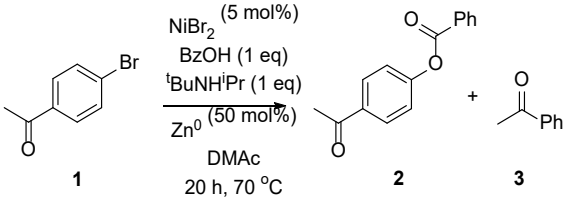

#	Deviation	Conv. (%)	**2** (%)	**3** (%)
1	-	100	81	9
2	In dark	100	76	13
3	2 eq BzOH and 2 eq ^{t}BuNH^{i}Pr	100	89	6
4	5 mol% dtbbpy	100	61	38
5	40 °C	15	12	2
6	$Ni(OBz)_2$	100	83	15
7	DMF as solvent	21	19	2
8	$Bu_4N(OBz)$ as substrate	21	7	5
9	2 eq ^{t}BuNH^{i}Pr	100	90	10

Conditions: Bromoacetophenone (200 mM) Benzoic Acid (200 mM), ^{t}BuNH^{i}Pr (200 mM) Nickel(II) bromide (5 mol%), Zinc (50 mol%), DMAc (6 mL), 20 hours, 70 °C. [a] Determined by GC analysis.

Interestingly, increasing the equivalents of BzOH and ^{t}BuNH^{i}Pr only gave a slight increase in the yield for **2** to 89% (Table 1, entry 3), in fair contrast to (dtbbpy)$NiBr_2$-catalyzed reactions which require non-equimolar ratios of carboxylic acid, base and aryl halide.[4,5,7,8,10,25–27] Addition of dtbbpy-ligand under optimized conditions showed a declined yield of ester **2** and an increased yield in acetophenone (**3**) as byproduct (Table 1, entry 4). Therefore, it is proposed that the addition of ligand slows down ligand exchange as elementary step causing the formation of protodehalogenated side product **3** (Figure 2, LE $k_{dtbbpy} < k_{LF}$). Nickel catalyzed carboxylate *O*-arylation using dtbbpy as ligand operate at mild temperatures (25–40 °C), but for the ligand-free reaction lowering the temperature to 40 °C had a detrimental effect on the formation of ester **2** (Table 1, entry 5), presumably due to the slower oxidative addition at a less electron-rich nickel center (Figure 2, OA: $k_{dtbbpy} > k_{LF}$). Further attempts to enable equimolar substrate ratios using the (dtbbpy)$NiBr_2$ system by changing the ligand (Table S5) or conditions (Table S8) were unproductive and lead us to pursue investigation of the ligand-free system. To gain structural insight into the complexes relevant to catalysis, the precursor was exchanged for nickel(II) benzoate, resulting in a comparable yield for ester **2** (Table 1, entry 6), indicating that at least for the initial reduction and oxidative addition a bromide ligand is not essential. Moreover, when DMAc (*N,N*-dimethylacetamide) as solvent is exchanged for DMF (*N,N*-dimethylformamide), greatly diminished yields are obtained (Table 1, entry 7). Due to the slight increase in steric bulk of DMAc, nickel halide systems in this solvent are significantly more dynamic than in DMF.[28]

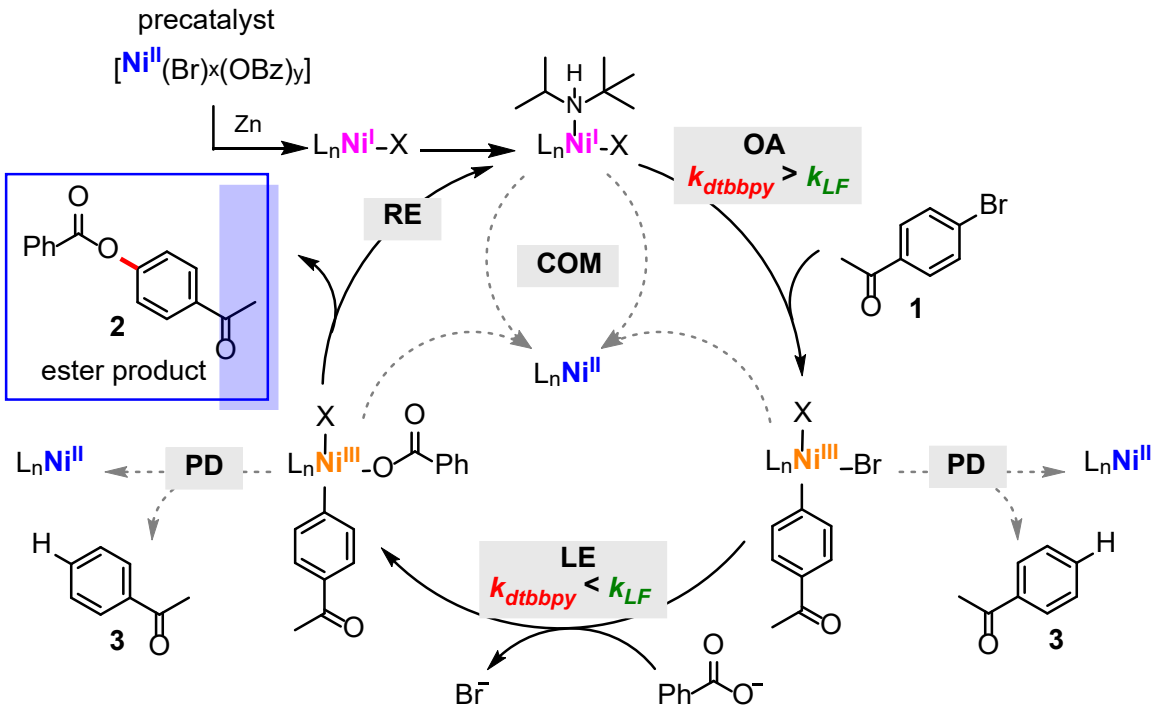

Figure 2. Mechanistic hypothesis of productive catalysis, protodehalogenation (side product formation) and comproportionation. OA, oxidative addition; LE, ligand exchange; RE, reductive elimination; PD, protodehalogenation; COM, comproportionation; *k*, rate; dtbbpy, 4,4'-di-tert-butyl-2,2'-bipyridine; LF, ligand-free.

Furthermore, the pivotal role of an aliphatic alkylamine base in catalysis, especially ^{t}BuNH^{i}Pr, was demonstrated by the use of other nitrogen-containing bases, which all provide inferior results with yields under 10% (Table S2, entries 4-6). Likewise, the use of tetrabutylammonium benzoate (Bu_4NOBz), rather than ^{t}BuNH^{i}Pr and benzoic acid, gave only 7 % yield for ester **2** (Table 1, entry 8). This result varies from (dtbbpy)$NiBr_2$-catalyzed reaction, with zinc as reducing agent, which does tolerate this substrate.[10] Adding an additional equivalent of ^{t}BuNH^{i}Pr increased the yield of ester **2** to 90% (Table 1, entry 9). These results clearly indicate a more elaborate role for ^{t}BuNH^{i}Pr than solely functioning as a Brønsted base, and therefore the catalytically active complex is proposed to be of the form [(^{t}BuNH^{i}Pr)Ni^{I}(L)$_n$] (Figure 2, where L = Br^-, BzO^-, DMAc). Summarizing the catalytic experiments, we propose that in absence of the dtbbpy-ligand, protodehalogenation and deleterious comproportionation reactions are prevented because of facile ligand exchange and reductive elimination steps (Figure 2). This enables the formation of *O*-aryl esters from equimolar amounts of coupling partners. In contrast, for the (dtbbpy)$NiBr_2$-catalyzed reaction an excess of carboxylate substrate is required to enhance the rate of ligand exchange and prevent unproductive comproportionation of Ni^{I} and Ni^{III}. However, for this reaction the rate of oxidative addition is expected to be higher due to the electron-donating effect of the dtbbpy ligand, and hence catalysis can be performed at a lower reaction temperature (Table S8).[10] Therefore, the ligand-free system shows diminished activity at 40 °C (Table 1, entry 2) whereas the (dtbbpy)$NiBr_2$-catalyzed reaction is less effective at elevated temperatures.

Spectroscopic investigation. To elucidate the nature of the Ni^{II} precatalyst and catalytic intermediates under ligand-free conditions we performed spectroscopic studies. UV-Vis spectra of the catalytic reaction mixture (Figure 3A, orange trace) and a DMAc solution containing $NiBr_2$, ^{t}BuNH^{i}Pr and BzOH (Figure 3A, green trace) proved to be identical, disclosing a Ni^{II} resting state. Additionally, a DMAc solution containing $NiBr_2$ and tetrabutylammonium benzoate (Bu_4NOBz) also gave a fairly similar UV-Vis spectrum (Figure 3A, purple trace), indicating the amine base does not coordinate to nickel. That the amine base primarily exists in the protonated, and the benzoic acid in the deprotonated form was further demonstrated via ^{1}H and ^{13}C NMR studies using ^{13}C-labeled benzoic acid (Figure S14, S15 and Figure 3B).[29] Comparison of the chemical shifts of BzOH-α-^{13}C (167.0 ppm), BzO^--α-^{13}C (168.9 ppm) and a mixture of $NiBr_2$, ^{t}BuNH^{i}Pr and BzOH in DMAc (~169.2 ppm) indicates that during catalysis the nucleophile is present as benzoate (Figure 3B; I, III and IV). The line broadening of the signal at ~169.2 ppm can be explained by the benzoate molecule being in close proximity to the paramagnetic Ni^{II} center and/or exchange between free and coordinated benzoate (Figure 3B; IV). Additionally, the chemical shift of the DMAc-α-C provides information about the role of DMAc as a ligand. While coordination of DMAc was observed for solely $NiBr_2$ (~171 ppm) in DMAc, DMAc serves a minor role as a ligand (169.2 ppm) for the mixture containing all components (Figure 3B; II and IV).

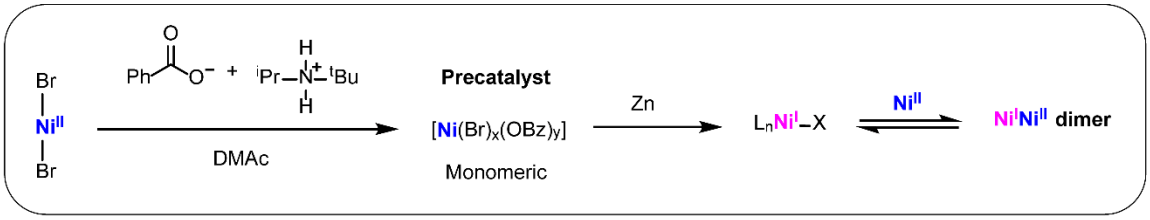

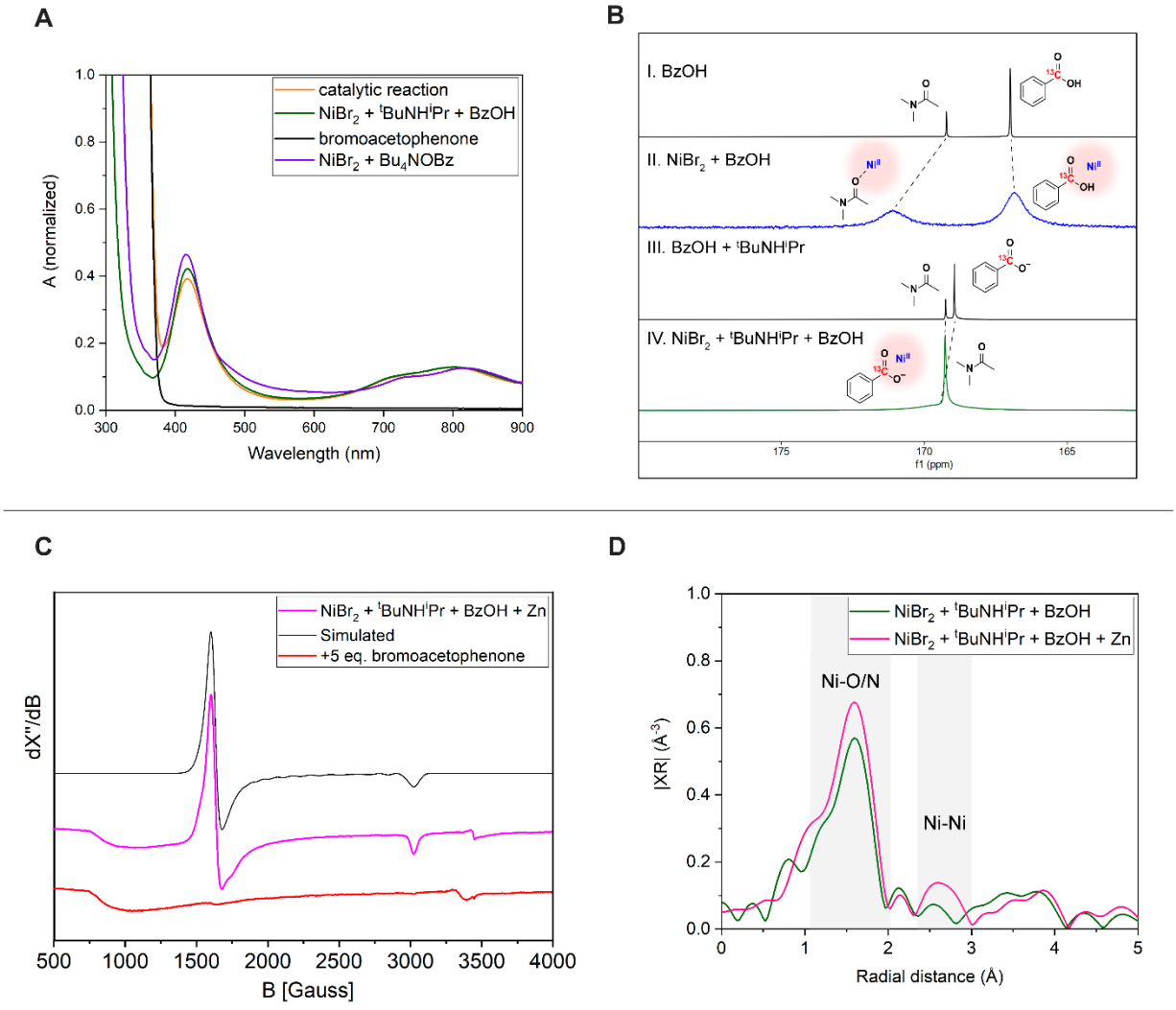

Figure 3. Spectroscopic investigations on the nickel system. [A] UV-Vis spectra in DMAc, catalytic reaction after 2h (at 9% yield of 2). [B] ^{13}C NMR spectra in DMAc. [C] X-Band EPR spectra at 10K. [D] Ni K-edge k^2-weighted Fourier transform EXAFS spectrum of frozen DMAc solution.

For further structural characterization we turned to X-ray absorption spectroscopy (XAS), since Ni K-edge XAS has shown to be a valuable spectroscopic tool for the elucidation of the local structure including geometry of molecular coordination complexes as well as their electronic structures.[30–32] For a DMAc solution containing $NiBr_2$, ^{t}BuNH^{i}Pr and BzOH the X-ray absorption near edge structure spectrum (XANES) (Figure S18) reveals a distinct pre-edge peak at 8333 eV which can be assigned to a 1s → 3d electronic transition, while the 1s → 4p$_z$ electronic transition (expected at 8337 eV) is absent thereby excluding the formation of complexes lacking one or more axial ligands (square planar and square pyramidal geometries).[33] More structural parameters were determined by Extended X-ray absorption fine structure (EXAFS) analysis, with figure 3D providing the Fourier Transform (FT) EXAFS function. The absence of any remote nickel shell, as observed for a DMAc solution containing only $NiBr_2$ and ^{t}BuNH^{i}Pr (Figure S21), is

indicative for monomeric nickel complexes present in solution with 1.9(1) Ni–O/Ni–N at 2.08(2) Å (Figure 3D, green trace, for details see S.I.). However, solely based on nickel K-edge EXAFS data an exact coordination number of the bromide shell cannot be determined reliably due to the almost complete anti-phase behavior of different Ni–Br contributions, when present at slightly different distances (Figure S23 – S24).[34] This means that these EXAFS data suggest that either no Ni–Br contributions are present, or that an even number of Ni–Br contributions (at different distances) are present. In order to provide more detail hereon, follow-up studies could include additional bromine K-edge XAS measurements.[32,35] To summarize, ^{t}BuNH^{i}Pr was found to be essential in catalytic experiments, while our spectroscopic investigations indicate that the Brønsted base primarily exists in the protonated form (^{t}BuNH$_2^{i}$Pr^{+}). We therefore propose that the bulk of the nickel that forms the precatalyst is present as a mixture of monomeric complexes of the type [Ni(Br)$_x$(OBz)$_y$].

More insight into the reduction of the formed Ni^{II} species was obtained stirring a Ni^{II}-precursor solution (a DMAc solution containing NiBr$_2$, ^{t}BuNH^{i}Pr and BzOH) in the presence of excess zinc.[36] The *in situ* reduced Ni^{II}-precursor solution was studied by UV-Vis, EPR and XAS spectroscopy. In the UV-Vis spectrum a new band at 541 nm is observed, as well as a shoulder at ~415 nm originating from non-reduced Ni^{II} (Figure S13, pink trace). EPR spectroscopy on this solution provided a spectrum with a characteristic S = 3/2 signal (Figure 3C, pink trace, for simulation details see Figure S16). Based on Ni K-edge XANES data the formation of complexes deprived of axial ligands (square pyramidal or square planar geometries) can be excluded (Figure S18). EXAFS analysis indicates an increase in the Ni–O/Ni–N shell (3.1(3)) at a bond distance of 2.04(1) Å and, more importantly, the emergence of a Ni–Ni shell at 3.10(3) Å with a coordination number of 0.6(5) (Figure 3D, pink trace, for details see SI). Overall, it can be rationalized that Ni^{II} is reduced by zinc to Ni^{I} which subsequently forms a bimetallic nickel intermediate. The trapping of formed Ni^{I} by excess Ni^{II} in solution leading to a Ni^{I}–Ni^{II} dimer was also reported by Nocera and co-workers in the nickel-catalyzed aryl etherification by (dtbbpy)NiCl$_2$ in the presence of quinuclidine and a photocatalyst or zinc.[14] Dimeric nickel complexes have been identified before as important intermediates in nickel-catalyzed cross-coupling, but this represents the first observation of a Ni^{I}–Ni^{II} dimer under ligand-free conditions.[14,20,21]

Next, the reactivity of the *in situ* formed Ni^{I}–Ni^{II} dimer was examined. Therefore we treated the pink-colored nickel solution, obtained after reduction, with 5 equiv. of 4'-bromoacetophenone and heated to 70 °C which resulted in a yellow-colored reaction mixture after 30 min (no color change was observed at R.T.). UV-Vis and EPR spectroscopy revealed the complete disappearance of the UV-Vis band at 541 nm (Figure S13, red trace) and the S = 3/2 signal in the EPR spectrum (Figure 3C, red trace). The catalytic relevance of the Ni^{I}–Ni^{II} dimer was further evaluated in an experiment, where NiBr$_2$ in the presence of ^{t}BuNH^{i}Pr and BzOH, was first reduced with zinc for 3 hours (see Figure S12 for UV-Vis spectrum). Next, this solution was filtered, to remove zinc, and 20 equiv. of bromoacetophenone were supplied and the mixture was stirred at 70 °C for 30 min. Subsequent GC analysis revealed minor formation of *O*-aryl ester **2** (yield <2%). Diminishing the reduction time to 30 min. (see Figure S12 for UV-Vis spectrum), resulted in no ester product **2** formation. Moreover, this experiment was repeated but now besides bromoacetophenone also another 0.5 equiv. of zinc was added after filtration. After 20 hours reaction time at 70 °C ester **2** was obtained in 80% yield. These results are notable since it contrasts with other studies into nickel-catalyzed C-heteroatom bond formations, where: 1) dimeric nickel complexes proved to be unreactive towards aryl halides[19,20] or 2) high concentrations of low-valent nickel had a detrimental effect due to the facile formation of inactive states such as nickel black, Ni^{II} or Ni^{I}–Ni^{I} dimers.[14,24] This is also highlighted by the numerous literature reports on successful marriages between photocatalysis and nickel catalysis, as photocatalytic reduction of nickel ensures a low absolute concentration of Ni^{I}, suppressing deleterious pathways.

To demonstrate the applicability of the developed protocol for ligand-free nickel-catalyzed ester bond formation with equimolar amounts of aryl halide, carboxylic acid and base we examined the scope of this reaction (Figure 4). Changing the aryl bromide from **1** (81%) to 4'-iodoacetophenone **5** gave the corresponding ester product **2** in a good yield (87%). Even when using aryl chloride **6**, catalytic product formation was observed albeit with lowered yields (21%). Aryl halides lacking sufficient electron-withdrawing groups show low reactivity (**8, 9, 10**) presumably because of a slow rate for oxidative addition. A variety of electron-poor aryl bromides were found to be effective coupling partners (**11-15**). For the carboxylic acid coupling partner, sterically hindered pivalic acid and cyclohexanecarboxylic acid (**16, 17**) furnished the corresponding ester efficiently, as well as various aromatic carboxylic acids (**19-21**). Only acetic acid hampered catalysis and afforded the ester product (**18**) in poor yield (<10%).

To provide an opening for future studies into photocatalyzed nickel carboxylate *O*-arylation, we investigated the herein developed ligand-free system under photocatalytic conditions. Zinc was replaced by the competent photocatalyst (Ir(ppy)$_3$) which only furnished ester product **2** in moderate yields, also for a reaction with excess BzOH and ^{t}BuNH^{i}Pr (Table S6, entries 1 and 2) which is in contrast to the (dtbbpy)NiBr$_2$-catalyzed reaction (Table S6, entry 3).[4] Previous studies showed that in ligand-based systems, (dtbbpy)NiBr$_2$ directly quenches the excited photocatalyst and that ^{t}BuNH^{i}Pr has no function in the photocatalysis.[37,38] Moreover, in ligand-free C–N cross-coupling 1,4-diazabicyclo[2.2.2]octane (DABCO) is employed as a base and serves also as a quenching agent for the excited Ir^{III}* photocatalyst, being oxidized to generate Ir^{II} which consecutively reduces Ni^{II}.[17] However, for ligand-free carboxylate *O*-arylation the addition of DABCO diminished the formation of ester **2** (Table S6, entry 4).

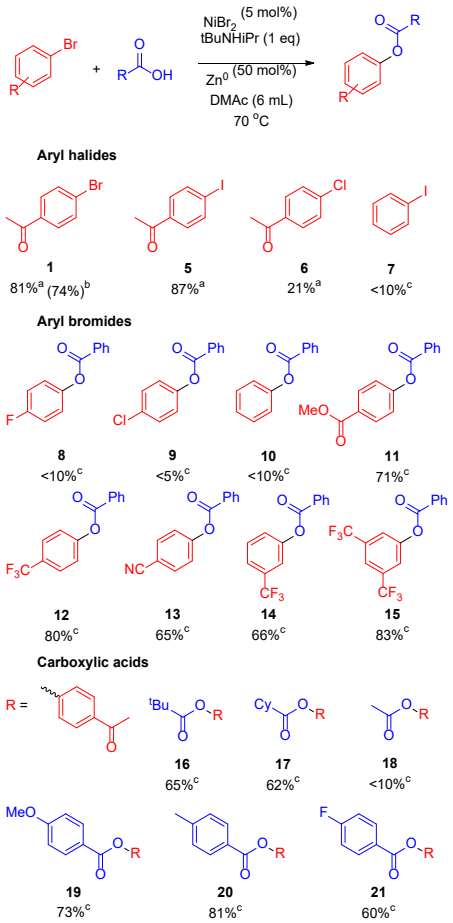

Figure 4. Substrate scope of $NiBr_2$-catalyzed esterification of carboxylic acids and aryl bromides. [a] Yield determined by GC with mesitylene as internal standard after 20 hours reaction time. [b] Isolated yield. [c] Yield determined by ^1H NMR with 1,3,5-Tri-tert-butylbenzene as internal standard after 24 hours reaction time.

The incompatibility of DABCO with ligand-free conditions was also displayed in a reaction with zinc as reducing agent, which resulted in no formation of ester **2** (Table S6, entry 5). This is presumably caused by coordination of DABCO inhibiting catalysis, similar to inhibition we observed by addition of COD as poison (Table S7, entry 6). Furthermore, photoinitiation with visible light (405 nm) afforded ester **2** only in moderate yields (Table S6, entries 6 and 7). These results show that it could be possible to enable equimolar photocatalytic ligand-free nickel-catalyzed carboxylate *O*-arylation, if a compatible quencher which preferably also serves as the base is found.

Summary & Conclusions

In summary, the here presented mechanistic studies of nickel-catalyzed carboxylate *O*-arylation have uncovered the competition between productive catalysis and off-cycle pathways (comproportionation and protodehalogenation) that exists for all fundamental elementary steps. In the absence of an exogenous dtbbpy-ligand these deleterious reactions were significantly suppressed allowing equimolar amounts of coupling partners. The spectroscopic investigation of this novel catalytic system revealed that during catalysis the bulk of Ni^{II} is present in the form of $[Ni(Br)_x(OBz)_y]$, yet for catalysis an alkylamine base was essential. Studies into the reduction of the Ni^{II}-precursor identified a bimetallic pathway resulting in a catalytically relevant Ni^{I}–Ni^{II} dimer. The presented insights into the reaction pathways of the commonly proposed self-sustained Ni^{I}/Ni^{III} catalytic cycle reveal that for carboxylate *O*-arylation a choice must be made between either mild conditions or equimolar ratios of substrates. Thereby, we believe this knowledge will be relevant for the design of novel efficient nickel-catalyzed C-heteroatom bond formations under mild conditions.

Acknowledgments

This work is part of the Advanced Research Center for Chemical Building Blocks, ARC CBBC, which is co-founded and co-financed by the Netherlands Organization for Scientific Research (NWO, contract 736.000.000) and the Netherlands Ministry of Economic Affairs and Climate.

References

(1) Wenger, O. S. Photoactive Nickel Complexes in Cross-Coupling Catalysis. *Chem. - A Eur. J.* **2021**, *27* (7), 2270–2278.

(2) Zhu, C.; Yue, H.; Jia, J.; Rueping, Nickel-Catalyzed C-Heteroatom Cross-Coupling Reactions under Mild Conditions via Facilitated Reductive Elimination. M. *Angew. Chemie - Int. Ed.* **2021**, *60* (33), 17810–17831.

(3) Diccianni, J. B.; Diao, T. Mechanisms of Nickel-Catalyzed Cross- Coupling Reactions. *Trend Chem.* **2019**, 1–15.

(4) Welin, E. R.; Le, C.; Arias-Rotondo, D. M.; McCusker, J. K.; MacMillan, D. W. C. Photosensitized, energy transfer-mediated organometallic catalysis through electronically excited nickel(II). *Science* **2017**, *355* (6323), 380–385.

(5) He, M.; Yang, S.; Yu, X.; Bao, M. 7,10-Dibromo-2,3-dicyanopyrazinophenanthrene Aggregates as a Photosensitizer for Nickel-Catalyzed Aryl Esterification. *Synlett.* **2021**, *32*, A-E.

(6) Zhu, D. L.; Li, H. X.; Xu, Z. M.; Li, H. Y.; Young, D. J.; Lang, J. P. Visible light driven, nickel-catalyzed aryl esterification using a triplet photosensitiser thioxanthen-9-one. *Org. Chem. Front.* **2019**, *6* (14), 2353–2359.

(7) Pieber, B.; Malik, J. A.; Cavedon, C.; Gisbertz, S.; Savateev, A.; Cruz, D.; Heil, T.; Zhang, G.; Seeberger, P. H. Evidence for Photocatalyst Involvement in Oxidative Additions of Nickel-Catalyzed Carboxylate O-Arylations. *Angew. Chemie - Int. Ed.* **2019**, *58* (28), 9575–9580.

(8) Lu, J.; Pattengale, B.; Liu, Q.; Yang, S.; Li, S.; Huang, J.; Zhang, J. Donor–Acceptor Fluorophores for Energy-Transfer-Mediated Photocatalysis. *J. Am. Chem. Soc.* **2018**, *140* (42), 13719–13725.

(9) Mo, Y.; Lu, Z.; Rughoobur, G.; Patil, P.; Gershenfeld, N.; Akinwande, A. I.; Buchwald, S. L.; Jensen, K. F. Microfluidic electrochemistry for single-electron transfer redox-neutral reactions. *Science.* **2020**, *368* (6497), 1352–1357.

(10) Sun, R.; Qin, Y.; Nocera, D. G. General Paradigm in Photoredox Nickel-Catalyzed Cross-Coupling Allows for Light-Free Access to Reactivity. *Angew. Chemie - Int. Ed.* **2020**, *59* (24), 9527–9533.

(11) Kitano, H.; Ito, H.; Itami, K. Palladium-Catalyzed Esterification of Carboxylic Acids with Aryl Iodides. *Org. Lett.* **2018**, *20* (8),

2428–2432.
(12) Li, L.; Song, F.; Zhong, X.; Wu, Y. D.; Zhang, X.; Chen, J.; Huang, Y. Ligand-Controlled C?O Bond Coupling of Carboxylic Acids and Aryl Iodides: Experimental and Computational Insights. *Adv. Synth. Catal.* **2020**, *362* (1), 126–132.
(13) Shields, B. J.; Kudisch, B.; Scholes, G. D.; Doyle, A. G. Long-Lived Charge-Transfer States of Nickel(II) Aryl Halide Complexes Facilitate Bimolecular Photoinduced Electron Transfer. *J. Am. Chem. Soc.* **2018**, *140* (8), 3035–3039.
(14) Sun, R.; Qin, Y.; Ruccolo, S.; Schnedermann, C.; Costentin, C.; Nocera, D. G. Elucidation of a Redox-Mediated Reaction Cycle for Nickel- Catalyzed Cross Coupling. *J. Am. Chem. Soc.* **2019**, *141* (1), 89–93.
(15) Qin, Y.; Sun, R.; Gianoulis, N. P.; Nocera, D. G. Photoredox Nickel-Catalyzed C–S Cross-Coupling: Mechanism, Kinetics, and Generalization. *J. Am. Chem. Soc.* **2021**, *143* (4), 2005–2015.
(16) Yang, L.; Lu, H. H.; Lai, C. H.; Li, G.; Zhang, W.; Cao, R.; Liu, F.; Wang, C.; Xiao, J.; Xue, D. Light-Promoted Nickel Catalysis: Etherification of Aryl Electrophiles with Alcohols Catalyzed by a Ni^{II}-Aryl Complex. *Angew. Chemie - Int. Ed.* **2020**, *59* (31), 12714–12719.
(17) Till, N. A.; Tian, L.; Dong, Z.; Scholes, G. D.; MacMillan, D. W. C. Mechanistic Analysis of Metallaphotoredox C–N Coupling: Photocatalysis Initiates and Perpetuates Ni(I)/Ni(III) Coupling Activity. *J. Am. Chem. Soc.* **2020**, *142* (37), 15830–15841.
(18) Kawamata, Y.; Vantourout, J. C.; Hickey, D. P.; Bai, P.; Chen, L.; Hou, Q.; Qiao, W.; Barman, K.; Edwards, M. A.; Garrido-Castro, A. F.; Degruyter, J. N.; Nakamura, H.; Knouse, K.; Qin, C.; Clay, K. J.; Bao, D.; Li, C.; Starr, J. T.; Garcia-Irizarry, C.; Sach, N.; White, H. S.; Neurock, M.; Minteer, S. D.; Baran, P. S. Electrochemically Driven, Ni-Catalyzed Aryl Amination: Scope, Mechanism, and Applications. *J. Am. Chem. Soc.* **2019**, *141* (15), 6392–6402.
(19) Till, N. A.; Oh, S.; MacMillan, D. W. C.; Bird, M. J. The Application of Pulse Radiolysis to the Study of Ni(I) Intermediates in Ni-Catalyzed Cross-Coupling Reactions. *J. Am. Chem. Soc.* **2021**, *143* (25), 9332–9337.
(20) Mohadjer Beromi, M.; Brudvig, G. W.; Hazari, N.; Lant, H. M. C.; Mercado, B. Q. Synthesis and Reactivity of Paramagnetic Nickel Polypyridyl Complexes Relevant to C(sp2)–C(sp3) Coupling Reactions. *Angew. Chemie - Int. Ed.* **2019**, *58* (18), 6094–6098.
(21) Ting, S. I.; Williams, W. L.; Doyle, A. G. Oxidative Addition of Aryl Halides to a Ni(I)-Bipyridine Complex. *J. Am. Chem. Soc.* **2022**.
(22) Na, H.; Mirica, L. M. Deciphering the mechanism of the Ni-photocatalyzed C–O cross-coupling reaction using a tridentate pyridinophane ligand. *Nat. Commun.* **2022**, *13* (1), 1–11.
(23) Corcoran, E. B.; Pirnot, M. T.; Lin, S.; Dreher, S. D.; Dirocco, D. A.; Davies, I. W.; Buchwald, S. L.; Macmillan, D. W. C. Aryl amination using ligand-free Ni(II) salts and photoredox catalysis. *Science.* **2016**, *353* (6296), 279–283.
(24) Gisbertz, S.; Reischauer, S.; Pieber, B. Overcoming limitations in dual photoredox/ nickel-catalysed C–N cross-couplings due to catalyst deactivation. *Nat. Catal.* **2020**, *3* (8), 611–620.
(25) Zhu, D. L.; Li, H. X.; Xu, Z. M.; Li, H. Y.; Young, D. J.; Lang, J. P. Visible light driven, nickel-catalyzed aryl esterification using a triplet photosensitiser thioxanthen-9-one. *Org. Chem. Front.* **2019**, *6* (14), 2353–2359.
(26) Bortnikov, E. O.; Semenov, S. N. Coupling of Alternating Current to Transition-Metal Catalysis: Examples of Nickel-Catalyzed Cross-Coupling. *J. Org. Chem.* **2021**, *86* (1), 782–793.
(27) Zu, W.; Day, C.; Wei, L.; Jia, X.; Xu, L. Dual aminoquinolate diarylboron and nickel catalysed metallaphotoredox platform for carbon–oxygen bond construction. *Chem. Commun.* **2020**, *56* (59), 8273–8276.
(28) Koide, M.; Suzuki, H.; Ishiguro, S. Steric Interaction of Solvation and Sterically Enhanced Halogeno Complexation of Manganese(ll), Cobalt(ll) and Nickel(ll) Ions in N,N-Dimethylacetamide *J. Solution Chem.* **1994**, *23* (12), 1257–1270.
(29) Lundberg, H.; Tinnis, F.; Zhang, J.; Algarra, A. G.; Himo, F.; Adolfsson, H. Mechanistic Elucidation of Zirconium-Catalyzed Direct Amidation. *J. Am. Chem. Soc.* **2017**, *139* (6), 2286–2295.
(30) Hao, W.; Sha, Y.; Deng, Y.; Luo, Y.; Zeng, L.; Tang, S.; Weng, Y.; Chiang, C. W.; Lei, A. XANES/EPREvidenceofthe Oxidation of Nickel(II) Quinolinylpropioamide and Its Application in Csp^3-H Functionalization *Chem. - A Eur. J.* **2019**, *25* (19), 4931–4934.
(31) Rabeah, J.; Radnik, J.; Briois, V.; Maschmeyer, D.; Stochniol, G.; Peitz, S.; Reeker, H.; La Fontaine, C.; Brückner, A. Tracing Active Sites in Supported Ni Catalysts during Butene Oligomerization by Operando Spectroscopy under Pressure. *ACS Catal.* **2016**, *6* (12), 8224–8228.
(32) Feth, M. P.; Klein, A.; Bertagnolli, H. Investigation of the Ligand Exchange Behavior of Square-Planar Nickel(II) Complexes by X-ray Absorption Spectroscopy and X-ray Diffraction. *Eur. J. Inorg. Chem.* **2003**, No. 5, 839–852.
(33) Colpas, G. J.; Maroney, M. J.; Bagyinka, C.; Kumar, M.; Willis, W. S.; Suib, S. L.; Baidya, N.; Mascharak, P. K. X-ray Spectroscopic Studies of Nickel Complexes, with Application to the Structure of Nickel Sites in Hydrogenases. *Inorg. Chem.* **1991**, *30* (5), 920–928.
(34) Tromp, M.; Van Bokhoven, J. A.; Arink, A. M.; Bitter, J. H.; Van Koten, G.; Koningsberger, D. C. Cu K-Edge EXAFS Characterisation of Copper(I) Arenethiolate Complexes in both the Solid and Liquid State: Detection of Cu-Cu Coordination *Chem. - A Eur. J.* **2002**, *8* (24), 5667–5678.
(35) Evans, J.; Levason, W.; Perry, R. J. Nickel K-Edge Extended X-Ray Absorption Fine Structure Studies of Bis(diamine) Nickel-(ll) and -(III) Complexes. *J.Chem. Soc. Dalt. Trans.* **1992**, 1497–1501.
(36) Lin, Q.; Diao, T. Mechanism of Ni-Catalyzed Reductive 1,2-Dicarbofunctionalization of Alkenes. *J. Am. Chem. Soc.* **2019**, *141* (44), 17937–17948.
(37) Tian, L.; Till, N. A.; Kudisch, B.; MacMillan, D. W. C.; Scholes, G. D. Transient Absorption Spectroscopy Offers Mechanistic Insights for an Iridium/Nickel-Catalyzed C–O Coupling. *J. Am. Chem. Soc.* **2020**, *142* (10), 4555–4559.
(38) Ting, S. I.; Garakyaraghi, S.; Taliaferro, C. M.; Shields, B. J.; Scholes, G. D.; Castellano, F. N.; Doyle, A. G. ^{3}d-d Excited States of Ni(II) Complexes Relevant to Photoredox Catalysis: Spectroscopic Identification and Mechanistic Implications. *J. Am. Chem. Soc.* **2020**, *142*, 5800–5810.